Inactivation of common airborne antigens by perfluoroalkyl chemicals modulates early life allergic asthma

Mengjing Wang[a], Qianqian Li[b], Meifang Hou[c], Louisa L. Y. Chan[d], Meng Liu[d], Soo Kai Ter[d], Ting Dong[a], Yun Xia[d,1], Sanjay H. Chotirmall[d], and Mingliang Fang[a,1]

[a]School of Civil and Environmental Engineering, Nanyang Technological University, 639798 Singapore, Singapore; [b]Key Laboratory of Environmental Nanotechnology and Health Effects, Research Center for Eco-Environmental Sciences, Chinese Academy of Sciences, 100085 Beijing, China; [c]School of Ecological Technology and Engineering, Shanghai Institute of Technology, 201418 Shanghai, China; and [d]Lee Kong Chian School of Medicine, Nanyang Technological University, 639798 Singapore, Singapore

Edited by Catherine J. Murphy, University of Illinois at Urbana–Champaign, Urbana, IL, and approved April 29, 2021 (received for review June 11, 2020)

Allergic asthma, driven by T helper 2 cell-mediated immune responses to common environmental antigens, remains the most common respiratory disease in children. Perfluorinated chemicals (PFCs) are environmental contaminants of great concern, because of their wide application, persistence in the environment, and bioaccumulation. PFCs associate with immunological disorders including asthma and attenuate immune responses to vaccines. The influence of PFCs on the immunological response to allergens during childhood is unknown. We report here that a major PFC, perfluorooctane sulfonate (PFOS), inactivates house dust mite (HDM) to dampen 5-wk-old, early weaned mice from developing HDM-induced allergic asthma. PFOS further attenuates the asthma protective effect of the microbial product lipopolysaccharide (LPS). We demonstrate that PFOS prevents desensitization of lung epithelia by LPS, thus abolishing the latter's protective effect. A close mechanistic study reveals that PFOS specifically binds the major HDM allergen Der p1 with high affinity as well as the lipid A moiety of LPS, leading to the inactivation of both antigens. Moreover, PFOS at physiological human (nanomolar) concentrations inactivates Der p1 from HDM and LPS in vitro, although higher doses did not cause further inactivation because of possible formation of PFOS aggregates. This PFOS-induced neutralization of LPS has been further validated in primary human cell models and extended to an in vivo bacterial infection mouse model. This study demonstrates that early life exposure of mice to a PFC blunts airway antigen bioactivity to modulate pulmonary inflammatory responses, which may adversely affect early pulmonary health.

early life exposure | pulmonary immunomodulation | perfluorinated chemicals | house dust mites | lipopolysaccharide

Allergic asthma is very common in children, and its incidence is increasing worldwide with urbanization (1–3). Asthma, which is characterized by eosinophilic airway inflammation, goblet cell metaplasia, and bronchial hyperreactivity, involves innate and adaptive immune responses to inhaled antigens such as the ubiquitous indoor allergen house dust mite (HDM), which signals via pattern recognition receptors on barrier epithelial cells (ECs) and dendritic cells (DCs) (2, 4). Abundant evidence shows that HDM is one of the most important sources of allergenic triggers (5). The HDM component cysteine protease Der p1 generally serves as a surrogate of environmental exposure to HDM (6).

Accumulating evidence suggests that environmental encounters that occur during childhood can influence the risk of allergic sensitization (7). Epidemiological studies suggest that exposures to high numbers of microbes may protect against allergic asthma (8). The gram-negative bacterial membrane endotoxin lipopolysaccharide (LPS), which is the most potent microbe-associated molecular pattern molecule and TLR4 agonist, is present at high levels in air and dust, and the extent of LPS exposure negatively correlates with the risk of developing asthma (8–10). Chronic exposure to LPS up-regulates the expression of the negative regulatory protein A20 in airway ECs, thereby reducing their production of cytokines and chemokines in response to allergens that suppress DC recruitment and T helper 2 (Th2) immunity (11, 12). Moreover, the intestinal microbiota modulates allergic asthma, and a low abundance of intestinal LPS is associated with a high risk of airway inflammation (13).

Notably, urbanization is associated with increased contact with household materials, antimicrobials, and cleaning products, as well as with increased exposure to a multitude of diverse chemicals (14). For example, perfluoroalkyl chemicals (PFCs) are ubiquitous pollutants that are used in numerous industrial and consumer products (15). The half-lives in humans of the most common PFCs, perfluorooctane sulfonate (PFOS) and perfluorooctanoate (PFOA), are ≥4 y (16). These PFCs are commonly detected in the human serum (17). In the United States, PFCs can be detected in the blood of nearly every American, including the developing fetus, with mean serum concentrations of 20.7 and 3.7 ng/mL for PFOS and PFOA, respectively (18, 19). Children may have greater risk of exposure than teenagers and adults (20, 21), possibly because PFCs are transferred through the placenta (22) and have postnatal sources of exposure including human milk and house dust (23).

Significance

Perfluoroalkyl chemicals (PFCs) are man-made chemicals ubiquitously present in humans. We demonstrate that a major PFC, perfluorooctane sulfonate (PFOS), dampens mice from developing house dust mite (HDM)–induced asthma, while abolishing the microbial product LPS's protective effect in asthma development. This finding has direct human relevance, considering the low-PFOS concentrations necessary for its effect. Mechanistically, PFOS binds with high affinity to Der p1, a major allergen from HDM, as well as to the lipid A moiety of LPS, resulting in their inactivation. Our data highlight that PFC exposure may play a previously unappreciated role in modulating allergic asthma and emphasize the importance of reducing exposure.

Author contributions: M.F. designed research; M.W., Q.L., M.H., L.L.Y.C., M.L., S.K.T., T.D., Y.X., and S.H.C. performed research; M.W. and M.F. analyzed data; and M.W. and M.F. wrote the paper.

The authors declare no competing interest.

This article is a PNAS Direct Submission.

Published under the PNAS license.

[1]To whom correspondence may be addressed. Email: yunxia@ntu.edu.sg or mlfang@ntu.edu.sg.

This article contains supporting information online at https://www.pnas.org/lookup/suppl/doi:10.1073/pnas.2011957118/-/DCSupplemental.

Published June 7, 2021.

ENVIRONMENTAL SCIENCES

Downloaded at University of Liverpool on September 20, 2021

PFC exposure may influence the immune response to vaccination and allergies such as asthma. For example, the concentrations of PFOS in the sera of 587 5-y-old children are associated with decreased levels of vaccine antibodies (24). Robust epidemiological data demonstrate that the rates of asthma are increased in children with higher serum PFC concentrations (25, 26), which may be explained by alterations in TH1/TH2 polarization (toward the TH2 response) (27). Similarly, studies of murine models of asthma show that exposures to PFCs (≥milligram/kilogram) cause asthma-related outcomes such as airway hyperresponsiveness (AHR) and increased inflammation (28).

Thus, exposure to allergens and environment pollutants such as PFCs may profoundly affect the outcomes of asthma in children (29). Unfortunately, our understanding of how simultaneous exposures to these substances influence the direction of immune priming is insufficient. Here, we aimed, therefore, to determine the role of early life exposure to PFCs by testing different doses on the development of allergic asthma caused by exposure to PFOS, before allergen sensitization and challenge, as well how LPS prevents the induction of asthma. These findings suggest a mechanism in which exposure to PFCs during infancy play a previously unidentified role in modulating allergic asthma.

Results

Exposure to PFOS Inhibits HDM-Induced Allergic Asthma. According to the US Environmental Protection Agency's safe daily dose of PFOS (2×10^{-5} mg/kg/d), it is estimated that the North American and European populations are likely to experience ubiquitous and long-term uptake doses of PFOS ranging from 3 to 220 ng/kg/d (18, 21). To identify the effects of low-dose exposure to PFOS on early life allergic airway disease, we exposed 5-wk-old, weaned mice to low-dose (10 μg/kg) PFOS every other day for 2 wk (30) or to phosphate-buffered saline (PBS) before sensitization with HDM and the challenge (Fig. 1*A*). Noticeably lower numbers of eosinophils, neutrophils, and lymphocytes were detected in the PFOS-pretreated group (Fig. 1*B*).

Consistent with these finding, histopathological analysis revealed that mice pretreated with PFOS have reduced peribronchial and perivascular leukocyte infiltrates in the lung when exposed to HDM (Fig. 1*C*), verified by a lung inflammation score analysis (*SI Appendix*, Fig. S1). Similarly, periodic acid–Schiff (PAS) staining of these tissues from PFOS-pretreated groups detected abolished goblet cell hyperplasia and mucus production in airways in comparison with controls (Fig. 1*D*). Sera were analyzed for the levels of total IgE, HDM-specific IgE, IgG1, and IgG2a (Fig. 1*E*). Surprisingly, the total IgE level was significantly increased in the PFOS-pretreated group (Fig. 1*E*). Conversely, the levels of HDM-specific IgE and IgG1 were significantly lower compared with the PBS-treated group. To measure HDM-specific TH1/Th2 responses, we stimulated cells from mediastinal lymph nodes (MLNs) in vitro with HDM and found that PFOS reduced the production of Th2 cytokines (IL-5, IL-10, and IL-13) and a Th17 cytokine (IL-17) but increased the production of the Th1 cytokine IFN-γ by MLNs treated with HDM (Fig. 1*F*) and decreased AHR (Fig. 1*G*).

Exposure to PFOS Inhibits Early-Life, LPS-Induced Protection against Asthma. To investigate the effects of PFOS on LPS-mediated protection against asthma, we exposed mice every other day for 2 wk to 100-ng LPS, with or without PFOS (10 μg/kg), or to PBS before sensitization to HDM and the challenge. Airway inflammation and Th2 responses were significantly inhibited in mice pretreated with LPS, compared with untreated mice. In contrast, simultaneous exposure of mice to PFOS and LPS produced more eosinophils and neutrophils, compared with mice only exposed to LPS (Fig. 1*B*). The inflammatory infiltrates detected in H&E-stained lung sections (Fig. 1*C* and *SI Appendix*, Fig. S1), goblet cell hyperplasia, and mucus production (revealed by PAS staining) (Fig. 1*D* and *SI Appendix*, Fig. S1) of tissues isolated from the LPS+PFOS/HDM group were increased, compared with the LPS-treated group. We detected increased levels of total IgE and HDM-specific IgE and decreased levels IgG2a in mice pretreated with LPS+PFOS (Fig. 1*E*). We further found that MLN cells from mice pretreated with LPS+PFOS secreted significantly higher levels of IL-5 and IL-13 than MLN cells from mice only pretreated with LPS. Notably, the production of IL-17 increased and that of IFN-γ decreased (Fig. 1*F*). LPS+PFOS reversed the LPS-induced decrease in methacholine-induced AHR in mice immunized against HDM (Fig. 1*G*).

Exposure to PFOS Modulates Lung DCs Treated with HDM. Sensitization to HDM depends on DC subsets that migrate to the MLNs to prime $CD4^+$ T cell responses (31). When PBS-treated mice were challenged with HDM, conventional $CD11b^+$ DCs (cDCs), $CD103^+$ cDCs, and monocyte-derived DCs (moDCs) were recruited to the lungs (Fig. 1*H* and *SI Appendix*, Fig. S2). In mice pretreated with PFOS, fewer $CD11b^+$ DCs and moDCs were recruited, while the number of $CD103^+$ DCs was unaffected (Fig. 1*H*). Furthermore, simultaneous exposure of mice to HDM and PFOS diminished the LPS-induced deficiency in DC recruitment, and the numbers of both subsets of cDCs and moDCs increased with HDM stimulation, compared with mice pretreated with LPS (Fig. 1*H*). After exposure to HDM, PFOS inhibited the activation of DCs, consistent with reduced Th2 responses, as well as increased LPS-induced defective DC activation, consistent with restored Th2 responses.

Transcriptomic Analysis of PFOS-Induced Immunomodulation. We next performed RNA sequencing to understand the immunomodulatory effects of PFOS (Fig. 2 *A* and *B* and *SI Appendix*, Fig. S3). We identified differentially expressed genes (DEGs) in cells treated with PFOS, LPS, or both, which were then subjected to Gene Oncology enrichment analysis. We found that DEGs expressed at lower levels by the PFOS- and LPS-treated groups were mainly involved in the immune and defense responses (Fig. 2*C*). DEGs expressed at higher levels by the LPS/PFOS-treated group were similarly enriched, compared with the LPS-treated group.

Kyoto Encyclopedia of Genes and Genomes (KEGG) pathway analysis of the PBS-treated group revealed that the protective effect of LPS induced down-regulation of genes that encode components of the major histocompatibility class I pathway that mediates antigen presentation and processing (*SI Appendix*, Fig. S4). Down-regulated genes were activated upon simultaneous exposure to PFOS and LPS (*SI Appendix*, Fig. S4). Gene set enrichment analysis (GSEA) identified DEG sets in the PFOS- and LPS-pretreated groups that were significantly enriched in the KEGG term "TGF-beta signaling pathway," compared with the PBS-treated group, and enrichment of the LPS-treated group was the highest (Fig. 2*D*). GSEA also identified "ribosomes" as the significantly enriched pathway, compared with the LPS+PFOS– and LPS-treated groups. Weighted correlation network analysis further supports the conclusion that the "regulation of immune response" was the pathway that was significantly affected by LPS+PFOS and LPS pretreatment (*SI Appendix*, Fig. S5).

We further compared the expression of immune-related genes. Consistent with assays of murine models of asthma (11, 32), mice pretreated with PFOS expressed lower levels of genes involved in Th2 responses (Il4, Il5, Il10, and Il13), proinflammatory genes (Il6 and Tnf-α), mucin genes (Muc5ac and Muc5b), and activated Th1 responses (Ifn-γ), compared with those of the PBS-treated group (Fig. 2*E*). Simultaneous exposure to PFOS significantly up-regulated genes involved in Th2 responses (Il4 and Il5), inflammation (Il6), mucin synthesis (Muc5ac), and down-regulated Th1 responses (IFN-γ), compared with those of the LPS-protected group (Fig. 2*E*).

Downloaded at University of Liverpool on September 20, 2021

Fig. 1. Exposure to PFOS modulates early life allergic asthma in mice. (*A*) Dosing regimens of mouse treatment groups. Mice were preexposed to intranasal (IN) PFOS (10 μg/kg), LPS (100 ng), or with the same doses of LPS combined with PFOS every other day starting from −14 d, then intratracheally (IT) sensitized with 1-μg HDM on day 0 and challenged with daily 10-μg HDM daily from days 7 to 11. Mice were euthanized on day 14. (*B*) Cell numbers in BAL fluid. (*C*) Paraformaldehyde-fixed lungs were cut and stained with H&E. (*D*) Lung sections were stained with PAS to measure goblet cell hyperplasia and mucosal secretion in airways. (*E*) Enzyme-linked immunosorbent assay (ELISA) results for total IgE, HDM-specific IgE, IgG1, and IgG2a levels in sera. (*F*) MLNs were harvested, and single-cell suspensions were prepared. MLN cells were treated again for 3 d with medium containing HDM. The culture media were used for IL-5, IL-13, IL-17, IL-10, and IFN-γ ELISAs. (*G*) Airway hyperreactivity expressed as lung resistance (R_L). (*H*) Recruitment of DC subsets to the lungs. Data represent the mean ± SEM (n = 5 mice per group). $^*P < 0.05$, $^{**}P < 0.01$ (Mann–Whitney U test), n.s., not significant.

Downloaded at University of Liverpool on September 20, 2021

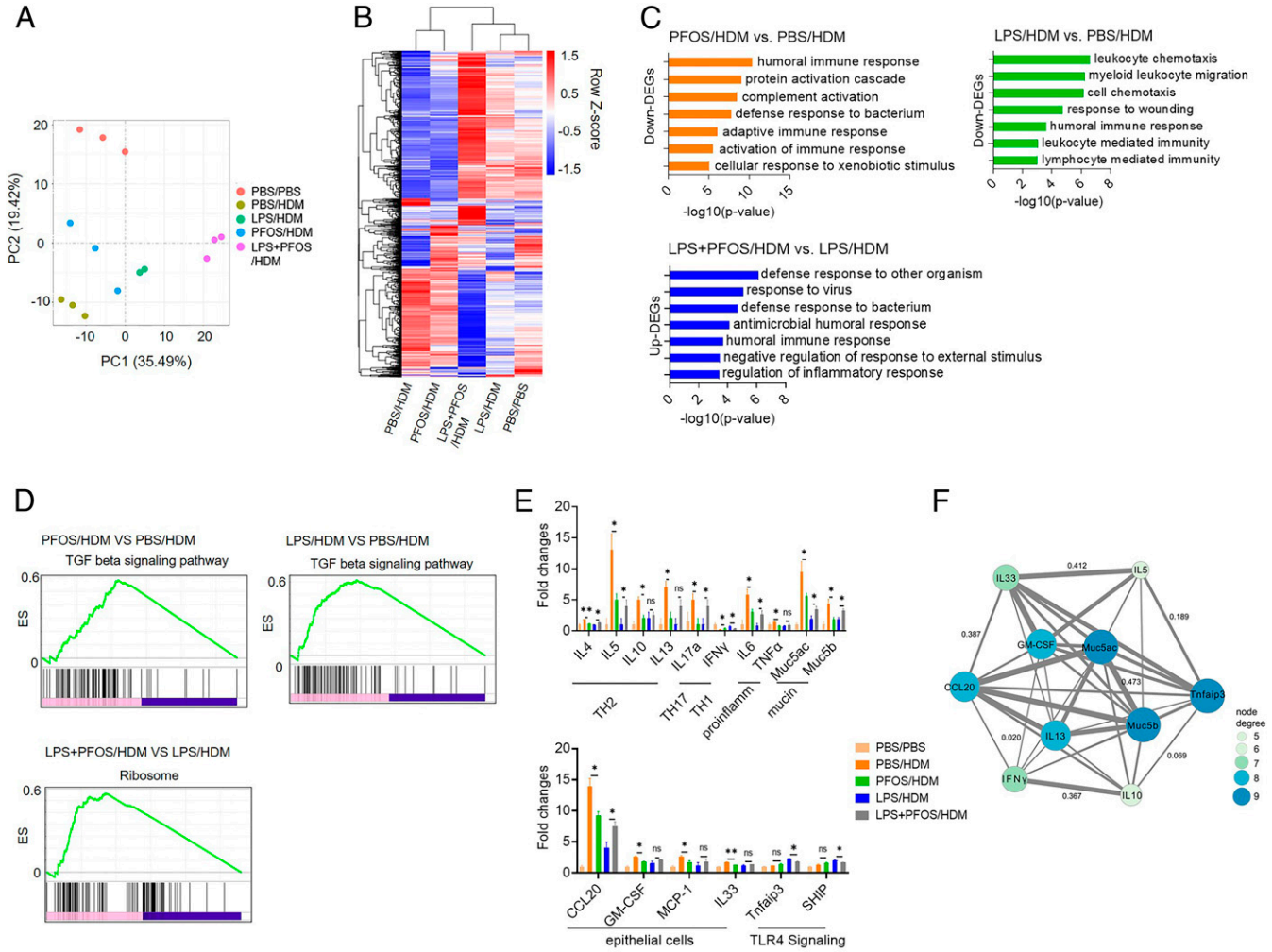

Fig. 2. Transcriptomic analysis of lungs of mice with HDM-induced asthma. (*A*) Principal component analysis of 15 samples according to normalized mRNA expression levels. (*B*) Hierarchical cluster analysis of common DGEs in the four treatment groups compared with the control PBS group. (*C* and *D*) GO enrichment (*C*) and GSEA (*D*) DEGs between the selected groups. (*E*) Effects of treatment on the expression levels of immune-related genes. Data are presented as the mean ± SEM of triplicates compared with the control PBS group. $*P < 0.05$, $**P < 0.01$ (ANOVA). (*F*) mRNA target network analysis of selected genes.

Upon allergen stimulation, lung ECs secret proallergic cytokines or chemokines to drive DC activation and therefore Th2-mediated immune responses (11, 33). Here, we found that lung homogenates from mice pretreated with PFOS, compared with controls, expressed reduced levels of Ccl20, Gm-csf, Mcp-1, and Il-33. These molecules are predominantly produced by lung ECs and are required for pulmonary allergic responses (Fig. 2*E*) (4). These results suggest that the number of lung ECs from PFOS-treated mice was reduced upon HDM stimulation. In contrast, the levels of Ccl20 messenger RNA (mRNA) in lung homogenates of LPS+PFOS/HDM mice were higher than in the LPS-treated group. The levels of Tnfaip3 (encoding A20) and Ship mRNAs, two negative regulators of TLR signaling, were downregulated in the lungs of HDM-treated mice exposed to PFOS/LPS (Fig. 2*E*), suggesting that they contribute to the increased responses. Among those genes, IL-5, IL-10, IL-13, IL-17, IFN-γ, Muc5ac, and Tnfaip3 were further consistently validated with RT-PCR (*SI Appendix*, Fig. S6).

Among 16 selected genes subjected to mRNA-target network analysis, 10 genes were significantly connected in our network (Fig. 2*F*). According to the size of each node, Muc5ac, Muc5b, and Tnfaip3 were significant nodes detected using network analysis, suggesting that they may play important roles in asthma, consistent with previous studies (34). Furthermore, early life exposure to low-dose PFOS (10 μg/kg) did not induce DEGs related to the activation of PPAR-α target genes, one major target of PFOS in previous studies (35, 36), suggesting that PFOS related PPAR-α pathway did not influence the outcome of the asthma-associated immune response. We therefore conclude that PFOS may regulate pulmonary inflammatory responses by decreasing the bioactivities of HDM and LPS.

PFCs Effectively Inactivate LPS In Vitro. To determine whether PFOS regulates allergic responses by modulating LPS bioactivity, we used PFOS and the top six most abundant PFCs in the sera of children to treat *Escherichia coli* LPS (*SI Appendix*, Fig. S7 and Table S2). Unexpectedly, these PFCs effectively inactivated LPS (Fig. 3*A* and *SI Appendix*, Fig. S8 and Table S3) using a concentration (1 nM) similar to that detected in human sera. Exposure to the seven PFCs tested with longer carbon chains and with a sulfonic group caused larger changes in LPS inactivation, suggesting a structure–function relationship. Higher concentrations of PFCs did not cause further inactivation. When we treated LPS with low-dose (1 nM) PFCs or with 1- to 100-nM PFOS for 6 h, inactivation was concentration and time dependent (Fig. 3 *B* and *C*).

Downloaded at University of Liverpool on September 20, 2021

Fig. 3. PFCs inactivate LPS in vitro. (*A*) *E. coli* LPS activity after incubation with PFCs. LPS bioactivity were measured using the LAL assay. (*B* and *C*) Validity and dynamics of LPS inactivation by PFCs. (*D*) Effects on PFOS on the activities of gut microbiome LPS, gram-negative LPS, and gram-positive LTA. (*E*) TEM images of the effects of PFOS on *E. coli* LPS. (Scale bar, 200 nm.) (*F*) Molecular dynamic (MD) simulations of the interactions between PFOS and LPS. LPS (polysaccharide is yellow and lipid A is red) and PFOS (carbon is cyan; oxygen is red; and fluorine and sulfur are green) shown as three-dimensional models. (*G*) Trajectories depicting the interaction between PFOS and LPS. PFOS interaction with LPS is gray and self-aggregated is cyan. (*H*) Effect of PFCs on cytokine production by THP-1 macrophages treated with LPS. (*I* and *J*) Effects of PFCs on LPS-induced activation of NF-κB (*I*) and PPAR-α (*J*) activation in THP-1 macrophages. (*K* and *L*) Effect of PFCs on cytokine production by A549 cells and HNECs (collected from three donors) treated with LPS. (*M*) Effects of treatment on the expression levels of immune-related genes in HNECs. Data are presented as the mean ± SEM of triplicates compared with the DMSO vehicle control (*A*–*D*, *J*, *L*, and *M*) or simultaneously treated with *E. coli* LPS (*H*, *I*, and *K*). $*P < 0.05$, $**P < 0.01$ (ANOVA).

Downloaded at University of Liverpool on September 20, 2021

We further tested the specificity of inactivation of LPS by PFCs. LPS from different bacteria differ in their effects on immune activation (7). Furthermore, the gram-positive bacterial product lipoteichoic acid (LTA) is a potent activator of the innate immune response (37). We found that PFOS differentially inactivated LPS prepared from *Pseudomonas aeruginosa* 10, *Salmonella enterica* serovar Typhimurium, *Klebsiella pneumoniae*, and *Proteus vulgaris*, as well as LTA prepared from *Bacillus subtilis* and *Entercoccus hirae* and the gut microbiome LPS (Fig. 3*D* and *SI Appendix*, Fig. S9 and Table S4). Significant inactivation was achieved at nanomolar concentrations. These results further suggest the relevance of these findings to humans.

PFCs Bind and Disaggregate *E. coli* LPS. To understand how PFCs inactivate LPS, LPS was titrated with the PFCs, and samples were observed using transmission electron microscopy (TEM). Intact LPS appeared as typical ribbon-like structures (Fig. 3*E*) (38). When LPS was treated with PFCs, the ribbon-like structure was not observed, and small spheres were visible instead (Fig. 3*E* and *SI Appendix*, Fig. S11), indicating that the LPS micelles were disaggregated. We conclude, therefore, that PFCs inactivated LPS by disrupting its structural integrity.

We used molecular dynamic simulations to analyze the interactions between LPS and PFCs. The PFCs bound LPS with a similar pattern, and the PFCs self-assembled into aggregates through hydrophobic interactions (Fig. 3*F* and *SI Appendix*, Fig. S12). Thus, the lipid A moiety of LPS wrapped through the perfluoroalkyl chains, and their hydrophilic groups formed hydrogen bonds with the polysaccharide moiety of LPS. The affinities of the PFC–LPS interactions were strongly dependent on the numbers of carbon atoms and functional groups, because the increasing the number of C–F groups contributed to the hydrophobic interactions, and the sulfonic headgroup of PFCs formed stronger hydrogen bonds with the self-assembled aggregates and LPS than the carboxylic headgroups (*SI Appendix*, Figs. S13 and S14). The formation of aggregated PFCs sterically hindered them from effectively binding the lipid A moiety (Fig. 3*G* and *SI Appendix*, Fig. S15), which may explain why the inactivation of PFOS was not strictly concentration dependent.

We used quantitative structure–activity relationship models to calculate 1,445 molecule descriptors of the test compounds to show that the electronegativity, atomic masses, and atomic van der Waals volumes were required for inactivation of LPS. Furthermore, molecular dynamic simulations revealed similar structural characteristics between the complexes of PFOS with different LPS and LTA molecules and that their binding affinities were generally consistent with their abilities to inactivate LPS in vitro (*SI Appendix*, Figs. S16 and S17).

PFCs Inhibit the Immunogenicity of *E. coli* LPS In Vitro. To further study the effects of PFCs on the immunogenicity of LPS in vitro, we first treated THP-1 macrophages with an LPS/PFOS mixture and measured the changes in the production of an inflammatory cytokine. TNF-α production was inhibited by the PFCs when the THP-1 cells were simultaneously treated with LPS (Fig. 3*H* and *SI Appendix*, Figs. S18 and S19). The levels of inhibition were generally consistent with their abilities to inactivate LPS.

The immunomodulatory effects of PFCs on THP-1 macrophages were not caused by cytotoxicity (*SI Appendix*, Fig. S20 *A* and *B*). Likewise, LPS-induced phosphorylation of NF-κB p65 was similarly inhibited by PFCs (100 nM) (Fig. 3*I*). PFCs alone did not have an effect (*SI Appendix*, Fig. S20*C*). Evidence indicates that the immune function of PFCs is mediated through PPAR-α (39), but we did not detect significant changes in PPAR-α expression (Fig. 3*G*), indicating that activation of PPAR-α may not a critical factor to initiate the immunomodulatory effects observed in THP-1 macrophages. Furthermore, LPS/PFOS-treated THP-1 macrophages were treated with the PPAR-α agonist ciprofibrate and antagonist GW6471, and both treatments did not have much effect on the PFOS-induced LPS inactivation, which implies that the direct PFOS–antigen interaction outweighs the PPAR-α pathway–induced immune response (*SI Appendix*, Fig. S21). These results suggest that PFCs affect the activation of NF-κB, which directly suppresses cytokine secretion by immune cells.

To further investigate the neutralization effect in modulating immune response, we have examined the treatment in both A549 cells and human primary nasopharyngeal ECs (HNECs). We also obtained a similar TNF-α decrease (Fig. 3 *K* and *L* and *SI Appendix*, Fig. S22), suggesting that PFOS-induced LPS neutralization and its associated immune modulation can be extended to human ECs. To determine the influence of PFOS in immune induction in LPS-stimulated HNEC, RNA sequencing was performed to characterize its gene expression change. Consistent with the result of asthma mouse models in the present study, we also found that most DEGs involved in the immune responses were down-regulated in the LPS/PFOS-treated group, compared with the LPS-treated group (*SI Appendix*, Fig. S23 *B* and *C*), including the "antigen processing and presentation" and ribosomes. For example, simultaneous exposure to PFOS and LPS expressed reduced levels of Il1β, Il8, Il-32, Tnf-α, Ccl20, Gm-csf, Il-33, and Tnfaip3, compared with those of the LPS-treated group (Fig. 3*M*).

PFOS Inhibits the *P. aeruginosa* Lung Infection In Vivo. To investigate whether we can extend this LPS neutralization effect by PFOS to the bacterial infection model, the immunosuppression potential of PFOS was examined in a live infection model of gram-negative *P. aeruginosa*. Mice were treated intranasally with PFOS (10 and 100 μg/kg/d) for 1 wk and then challenged with a dose of *P. aeruginosa* (1×10^7 colony-forming unit [CFU]). As shown in Fig. 4 and *SI Appendix*, Fig. S24, a significant reduction of numbers of eosinophils, neutrophils, and lymphocytes (Fig. 4*A*) was observed for the PFOS-pretreated group, compared with *P. aeruginosa* only. Consistently, proinflammatory cytokines, including IL-1β, IL-6, and TNF-α, in the bronchoalveolar lavage (BAL), lungs, and blood also exhibited a decreasing trend (Fig. 4 *B*–*D*), though they are not as dramatic as the changes in the LPS only versus LPS+PFOS in in vivo animals. Therefore, our results suggested that the immune depression effect of PFOS can be expanded to bacterial infection beyond the bacterial product LPS only.

PFOS Binds and Inactivates Der p1. We hypothesized that PFOS regulates allergic responses by modulating the biological activity of HDM. The cysteine protease Der p1, derived from the HDM *Dermatophagoides pteronyssinus*, is the major immunoactive component of the HDM tested here. Thus, we tested the effect of PFOS on Der p1. The concentration of PFOS was similar to that typically present in normal human sera (0.05 mg/mL). PFOS (1 nM) inactivated Der p1 by 22% (Fig. 5*A*). Isothermal titration calorimetry (ITC) showed that the binding affinity of the Der p1–PFOS interaction was 224 nM (Fig. 5*B*).

We propose a mechanism of proteolysis catalyzed by Der p1 (*SI Appendix*, Fig. S25) through which it inactivates a_1-antitrypsin through a thiol-dependent mechanism involving specific cleavage of the reactive center loop. Molecular docking and molecular–surface interaction analyses were used to identify the main PFOS binding sites within Der p1. PFOS occupied the active site of Der p1 through hydrogen bonding with His250 and Cys114 (Fig. 5 *C* and *D* and *SI Appendix*, Fig. S26). Molecular dynamic simulations further show that the sulfonic group of PFOS forms stable hydrogen bonds with active site residues (Fig. 5*E* and *SI Appendix*, Fig. S27). These conformations are consistent with the results of the molecular docking analysis. The distribution of PFOS around Der p1 was further found to involve the formation of PFOS aggregates using molecular dynamic analysis, which limit interactions with the active site (Fig. 5*F* and *SI Appendix*, Fig. S28), similar to the binding modes of PFC/LPS complexes.

Downloaded at University of Liverpool on September 20, 2021

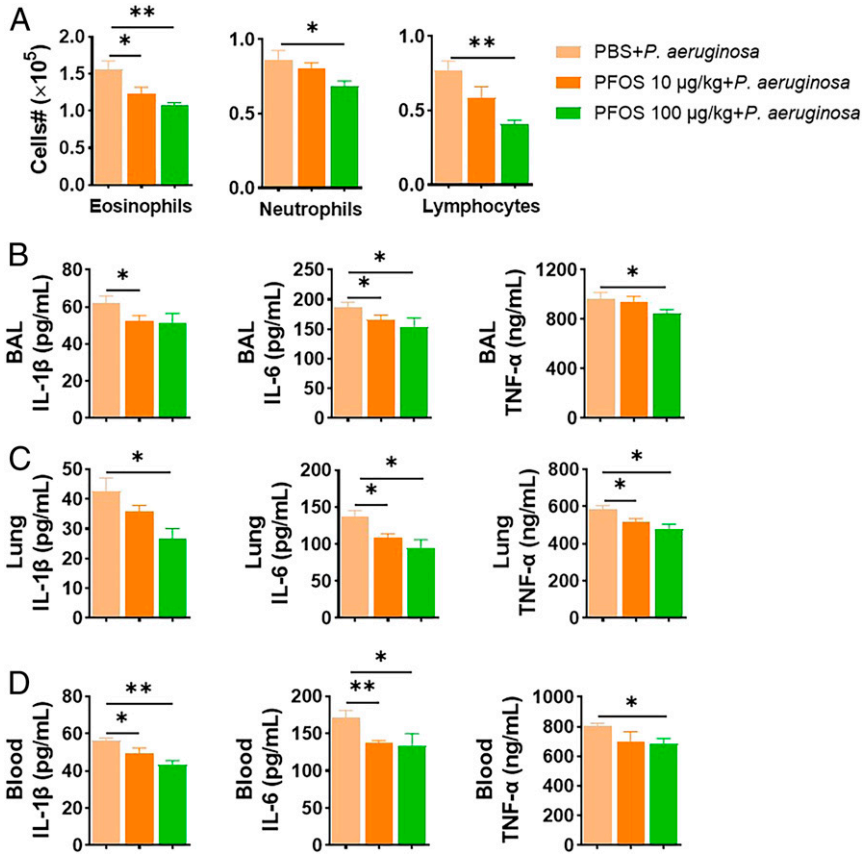

Fig. 4. PFOS inhibits mouse *P. aeruginosa* infection. Mice were preexposed to intranasal PFOS (10 and 100 μg/kg) for 1 wk, then intranasally with 10^7 CFU of *P. aeruginosa*. Mice were euthanized 24 h after the infection. (*A*) Cell numbers in BAL fluid. (*B–D*) Proinflammatory cytokines, including IL-1β, IL-6, and TNF-α, from the BAL (*B*), lung (*C*), and blood (*D*). Data represent the mean ± SEM (n = 5 mice per group). *$P < 0.05$, **$P < 0.01$ (ANOVA).

Discussion

Numerous studies suggest an association between exposure to PFCs and immunotoxicity, as manifested by suppressed immune function, lower vaccine effectiveness, airway hypersensitivity, and a greater risk of autoimmune diseases (28). The increasing rate of childhood asthma over recent decades, particularly in urban areas, indicates a larger role of environmental factors such as PFCs (40). Indeed, elevated PFCs can be a possible contributing factor in childhood asthma onset (25, 26). In contrast, a promising strategy to reduce the prevalence of asthma involves using microbial compounds to induce nonspecific tolerance during early infancy (11). Studies of mouse models show that early life exposure to LPS protects against the induction of asthma, which strongly supports the hygiene hypothesis (41). Although children are frequently affected by PFC toxicity and asthma, insufficient data are available to link PFCs to the early stages of asthma. Our present findings strongly support the possibility of an interaction between LPS-induced effects with immunological responses caused by exposure to PFCs.

Here, we show that mice treated with a low dose of PFOS inhibit HDM-induced allergic asthma. Compared with PBS-treated mice, PFOS-treated mice exhibited reduced eosinophilic airway inflammation, diminished airway goblet cell hyperplasia and mucus production, and decreased reactivity. These observations are consistent with the conclusion that the activation of DCs was inhibited in mice treated with PFOS. We further found that lung ECs in PFOS-treated mice were refractory to HDM stimulation, which led to defective DC activation, as well as reduced Th2 responses. Moreover, MLN cells of the PFOS/HDM group secreted less IL-10 when treated again with HDM in vitro, suggesting that reduced HDM-induced allergic responses associated with PFOS/HDM treatment were/are not caused by enhanced Treg cell function (42).

We believe that our present findings indicate that the initial suppressive effect of PFOS inhibits the symptoms of early asthma. However, we predict that an overall adverse effect of PFOS exposure, manifested as an attenuated immune response, likely predisposes children to respiratory infection and leads to an exacerbated allergic response later in life. This may be explained by our findings that the serum concentrations of total IgE were higher in mice treated with PFOS and then exposed to HDM versus those of the controls. Similarly, when mice are preexposed to combustion-derived particles, they exhibit a reduced pulmonary immune response to the HDM but develop a severe allergic inflammatory response when challenged with allergens as adults (43). Thus, elevated total IgE concentrations observed early in life may contribute to heightened susceptibility to allergens later in life. The PFOS concentrations used here (80-μg/kg total administered dose [TAD]) were much lower than those of other earlier studies using rodents (44), and the limit of detection was ≥1-mg/kg TAD of PFOS.

These findings, considered together with the results of our transcriptomic analysis, suggest that, in mice pretreated with a low dose of PFOS, the activation of PPAR-α target genes was not affected, consistent with other studies that PFOS cannot upregulate the expression of PPAR-α target genes in the lung until the high dose of 5 mg/kg (35, 36). We therefore assumed that PFOS inhibits the innate immune response to HDMs by directly decreasing the bioactivity of the latter.

PFOS is mainly distributed in the liver and peripheral circulation because of its proteinophilic properties (45). The physicochemical

ENVIRONMENTAL SCIENCES

Downloaded at University of Liverpool on September 20, 2021

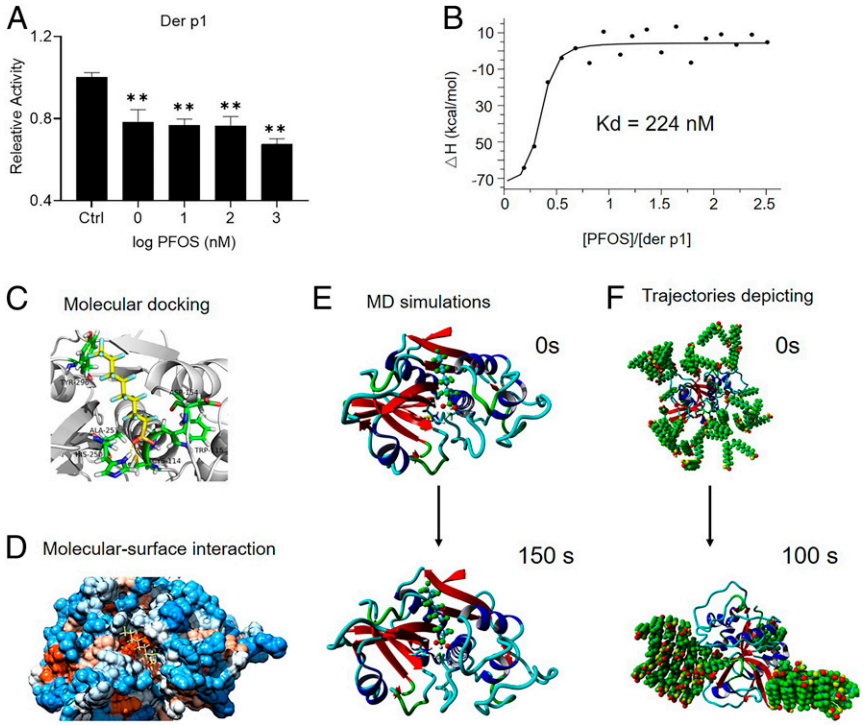

Fig. 5. PFOS inactivates Der p1. (*A*) Effect of PFOS on Der p1 activity. $*P < 0.05$, $**P < 0.01$ (ANOVA). (*B*) K_d values of the interaction between Der p1 and PFOS were determined using ITC. (*C*) Molecular docking analysis of the interactions between PFOS and Der p1. PFOS is shown in yellow, the protein is depicted in gray, and hydrogen bonds are indicated by the yellow dotted lines. (*D*) Molecular surface view of the interaction between PFOS and Der p1. The strongly hydrophobic region is orange; the weakly hydrophobic region is light orange; the strongly hydrophilic region is blue; and the weakly hydrophilic region is light blue. (*E*) Conformation of the complex formed between Der p1 and PFOS at 0 and 150 ns. (*F*) Trajectories depicting PFOS gathering around Der P1. PFOS is shown in green, and the protein is shown as a band.

properties of PFOS suggest that it interacts with the sulfonic acid group or the hydrophobic alkyl chain of Der p1. We found that PFOS bound Der p1 with dissociation constant at equilibrium (K_d) = 224 nM, compared with albumin, K_d = 80 nM, and the PFOS–liver fatty acid binding protein complex (K_d = 2,099 nM) (46, 47). In children with the highest serum concentrations of PFOS (207 nM), exposure to PFOS at nanomolar concentrations significantly inhibits human serum albumin and liver fatty acid binding protein in vitro (48, 49). These results suggest that investigators should focus on the potency of PFOS and how it influences the allergenic effects of HDM in humans.

Another important finding of the present study is that simultaneous exposure to LPS and PFOS abolished the protection conferred by the former upon infants against asthma. Compared with the protective effects of LPS, simultaneous exposure to PFOS and LPS increased eosinophilic airway inflammation, induced the development of airway goblet cell hyperplasia and mucus production, and increased airway hyper reactivity. PFOS prevented LPS-induced desensitization of lung ECs, thus restoring DC and Th2 activation. The anti-inflammatory effect of PFOS on the epithelium was further demonstrated in A549 cells and HNECs. Moreover, compared with the immune modulation of the PFOS-treated group, the LPS/PFOS group remained predisposed toward a TH1 cell-skewing environment, further confirming the potency with which PFOS inhibited the immunomodulatory effects of LPS to preclude these aspects of immune education.

This present study achieved an understanding of the immunomodulating effects of PFCs, which involved direct binding in vitro of PFCs and LPS. First, in the limulus amebocyte lysate (LAL) test, a direct protein–binding assay, there was no direct binding between PFCs and LPS, and PFCs alone did not induce an effect without LPS. Second, TEM analysis showed that PFCs shortened the typical LPS structure. Third, PFOA inhibits the induction of cytokine production to a greater extent when it is preincubated with LPS versus when PFOA and LPS are added together, as shown by a previous study (50). Fourth, we found that the inhibitory effects of PFCs on cytokine production by human immune cells occurred independently of PPAR-α activation but involves the inhibition of the activation of NF-κB. These findings are consistent with those of a previous study (51), which suggests that at environmentally relevant concentrations the effects of PFOS are independent of PPAR-α activation (50–52). Notably, when humans are exposed to multiple PFCs, the blood concentrations of these compounds may increase, because their half-lives are several years. Therefore, cross-talk between PFCs and LPS cannot be completely excluded, as several previous studies have linked PFCs' major target (PPAR-α) with NF-κB (53–55). If PFCs levels are high enough to activate PPAR-α, cross-talk with NF-κB may be important.

Additionally, we have extended PFOS's neutralization effect to bacterial infections, though the immunodeficiency is not as dramatic to the pure LPS only versus LPS+PFOS. However, because of the complexity of the bacterial infection processes, whether it is completely driven by the neutralization effect or by any other pathway cross-talk can still be investigated in the future. For example, one study in a mouse model shows that exposures to a high dose of PFCs (>10 mg/kg) directly inhibit the expansion of intestinal bacterial infection at an early phase in an AHR-dependent manner (56). In addition, besides microbial and microbial products (e.g., LPS), the immune response to airway viral is also critical for the protection against infection; how PFOS affects virus infection is unknown. Although a recent study reported mouse exposure to PFOS at 1.5 μg/kg/d for 4 wk does not affect influenza viral clearance and immune development

Downloaded at University of Liverpool on September 20, 2021

and function (57), further work is necessary to elaborate the meaning of PFOS–virus interaction.

Moreover, we show here a unique dose response associated with the interactions of PFOS and allergens. Thus, low-dose PFC exposure effectively inactivated Der p1 and LPS in vitro; however, a high dose of PFC did not increase inactivation. This may be explained by the partial antagonism of PFOS toward LPS and Der p1, such that binding will not completely block their immune functions. Alternatively, PFOS may aggregate at higher concentrations. The structure of Der p1 includes many loops, and LPS possesses many external hydrophobic regions that provide more available binding regions, which facilitate the generation of PFC aggregates during the interaction with Der p1 or LPS.

Indoor dust is a primary reservoir for indoor chemicals such as PFCs (58) and an important source of human exposure to LPS and HDM. Exposure of toddlers to these environmental pollutants via ingestion of dust may be more important than that acquired through eating, because of frequent hand-to-mouth movements (59). Thus, PFCs may potently inhibit the bioactivities of LPS and Der p1 present in house dust. Although numerous studies of the direct health effects of mixtures of environmental chemicals and allergens in house dust have been conducted (28, 60), identification of their potential interactions requires further investigation.

Furthermore, intestinal commensal bacteria regulate allergic asthma (61). LPS produced by the gut microbiome is one of the most potent activators of innate immune signaling and an important mediator of the microbiome's influence on host physiology (62). Our findings demonstrate that PFOS inactivated, with varying potencies, LPS and LTA from different bacterial species. PFOS is released into peripheral circulation after dietary exposure, and commensal LPS may be inactivated in the intestinal lumen. Furthermore, DCs and macrophages engulf LPS produced by commensal microbes that reside in the intestinal tract (63). LPS is further inactivated in different tissues, according to findings that PFCs are widely distributed in the circulation, liver, and lung (64). Thus, contact with a microbial environment during early life without an interaction with other environmental factors may not guarantee that the development of asthma will be prevented later in life.

Laboratory tests commissioned by the Environmental Working Group have found that PFC is likely present in all major water supplies in the United States (65). Very few toxicological studies investigated the health effects of the interplay between microbes and chronic exposure to environmentally or human-relevant doses of PFCs. Inactivation by PFCs of the key immune modulators LPS and Der p1 may provide an explanation of their associations with immunological diseases. The developing immune system may be particularly vulnerable to immunotoxicity during the earliest stages of life, so it is essential to protect children's health from PFCs during that time. Life-long simultaneous exposure to environmental chemicals and microbiome-derived LPS and Der p1 may affect immunity in more complex ways than previously appreciated.

The susceptibility to allergic asthma is most likely mediated through a complex interplay of environmental factors. These likely include immune responses to multiple, diverse exposomic components such as biotics (e.g., microbes) and abiotics (e.g., chemicals), and the timing of exposure may be critically important. Here, we demonstrate the prominent role of PFC in inactivating LPS and Der p1, thereby modulating susceptibility to respiratory infection and overall children's pulmonary health. Understanding how different exposomic components contribute to the pathogenesis of complex diseases such as asthma emphasizes the importance of reducing exposure to PFOS during early life.

Materials and Methods

Mouse Model of HDM-Induced Asthma. Female (5 wk old) BALB/c mice were purchased from Sippr-BK Laboratories, housed under specific pathogen-free conditions, and studied using protocols approved in accordance with the Animal Ethics Committee of the Research Center for Eco-Environmental Sciences, Chinese Academy of Sciences (AEWC-RCEES-2021001). The HDM-induced allergic asthma method was a modification of published protocol ref. 11. HDM (1 μg) was delivered intratracheally into anesthetized mice on day 0. Before the HDM challenge, mice ($n = 5$ mice, each treatment) were treated with intranasal PFOS (10 μg/kg), LPS (100 ng), or with the same doses of LPS combined with PFOS every other day starting from 14 d before the first HDM challenge. Intranasal administration of LPS and PFOS mimics the pathophysiology of children's asthma disease in mice. HDM sensitization and following the challenge induces a robust Th2 cell response and eosinophilic airway inflammation in mice. The control group of mice received intranasal doses of PBS. Mice received daily intranasal 10-μg doses of HDM from days 7 through 11, and the mice were euthanized on day 14. In sum, we treated mice as follows: PBS/PBS group, mice were treated with PBS during the whole phases; PBS/HDM group, mice pretreated with PBS before HDM instillation; PFOS/HDM group, mice pretreated with PFOS before HDM instillation; LPS/HDM group, mice pretreated with LPS before HDM instillation; and LPS+PFOS/HDM group, mice pretreated with the complex of LPS and PFOS before HDM instillation. BAL analysis, AHR, flow cytometric analysis, total IgE, HDM-specific antibodies, cytokine assays, lung histology, and transcriptomic analyses are described in *SI Appendix*.

Treatment with LPS and PFCs. LPS (100 ng/mL) isolated from *E. coli* 0111:B4 was incubated with PFCs for 6 h at 25 °C. LPS was used as a positive control. To determine the kinetics of LPS inactivation, we used human-relevant concentrations of PFCs. The test PFCs (1 nM each) were used to titrate purified *E. coli* LPS for 6 h at 25 °C. LPS purified from *E. coli* 0111:B4 (1, 10, 100, 1,000, and 10,000 ng/mL) was treated with 1 and 100 nM PFOS. All LPS samples were analyzed using an LAL assay, according to the manufacturer's instructions. In this assay, the LPS-activated protease cleaves the substrate to generate the chromogenic product p-nitroaniline. The detailed procedure is provided in *SI Appendix*.

TEM Analysis of the Structure of LPS. To measure the effect of the test PFCs on the native structure of LPS, LPS from *E. coli* 0111:B4 (5 mg/mL) in 0.1-M Tris·HCl (pH 7.2) was exposed to 1-mM PFCs for 6 h at 25 °C. The detailed procedure is provided in *SI Appendix*.

Quantitative Structure–Activity Relationship Model. A quantitative structure–activity relationship model was developed to analyze the inactivation potencies of PFCs relative to their structural and chemical characteristics. A model was built using theoretical molecular descriptor calculations, and the molecular descriptors were calculated using the PaDel descriptor. The detailed procedure is provided in *SI Appendix*.

Immune Stimulation In Vitro Assays Using Macrophage and Primary ECs. THP-1 macrophages, A549 cells, and HNECs were treated with PFOS, LPS, LPS+PFOS, and vehicle controls. Enzyme-linked immunosorbent assays were performed to determine the concentrations of TNF-α in culture supernatants. Cell viability tests were conducted using the alamarBlue assay. Western blot analysis and transient transfections assay were performed to measure the phosphorylation of p65 and PPAR-α in THP-1 macrophages. THP-1 macrophages were dosed with the PPAR-α agonist ciprofibrate and antagonist GW6471 to explore the role of the PPAR-α mechanism. A transcriptomic analysis was conducted using the HNEC cell. The detailed procedures are provided in *SI Appendix*.

***P. aeruginosa* Infection Post-1-wk PFOS Treatment.** All animal studies were conducted under protocols approved by the Animal Ethics Committee of the Research Center for Eco-Environmental Sciences, Chinese Academy of Sciences (AEWC-RCEES-2021001). Generally, females mount a stronger immune response than males; thus, groups of five female BALB/c mice (6 wk old, $n = 5$ for each treatment) were injected intranasally with PFOS (10 and 100 μg/kg body weight per day) for 1 wk before mice were intranasally infected with 10^7 CFU of *P. aeruginosa* strain 8821. Mice were euthanized 24 h after the infection. The control group of mice received intranasal doses of PBS. Another three groups were prepared alongside without any introduction of bacteria (i.e., PBS; 10 and 100 μg/kg body weight per day PFOS control). BAL analysis and cytokine assays are described in *SI Appendix*.

ENVIRONMENTAL SCIENCES

Downloaded at University of Liverpool on September 20, 2021

Treatment of HDM Allergen Der p1 with PFOS. PFOS was used to titrate the purified HDM allergen Der p1 (0.05 mg/mL) for 24 h at 25 °C. A MicroCal ITC 200 calorimeter was used to measure the K_d of PFOS bound to Der p1. The detailed procedure is provided in *SI Appendix*.

Molecular Docking Analysis to Identify the Interactions of PFOS with Der p1. We used AutoDock 4.2 to determine the binding modes of PFOS to Der p1. The detailed procedures and related parameters are described in *SI Appendix*.

Molecular Dynamic Simulation of the Interactions of PFOS with LPS, LTA, and Der p1. The computed conformations of complexes of PFOS with LPS, LTA, and Der p1 were further optimized using molecular dynamic simulation. Details of the molecular dynamic simulations, binding pattern analysis, and free energy of binding calculations are described in *SI Appendix*.

Statistical Analysis. Data presented as the mean ± SEM represent at least three independent experiments. For experiments using mice, we calculated the difference between groups using the Mann–Whitney *U* test for unpaired data (GraphPad Prism 8.0). The statistical significance of differences in vitro was assessed using two-way ANOVA. $P < 0.05$ indicates a significant difference. $EC_{20}/_{30}$ values were estimated using curves generated from the PFC inactivation data using a four-parameter sigmoidal dose–response model included with GraphPad Prism 8.0.

Data Availability. All data are included in the manuscript and/or *SI Appendix*.

ACKNOWLEDGMENTS. This work is supported by the Singapore Ministry of Education Academic Research Fund Tier 1 (04MNP000567C120), Nanyang Technological University Harvard School of Public Health Initiative for Sustainable Nanotechnology (M4082370.030), the Singapore National Environment Agency (M4061617), and Singapore Ministry of Health's National Medical Research Council under its Clinician–Scientist Individual Research Grant (MOH-000141), the Open Fund Individual Research Grant (OFIRG/0076/2018), the Lee Kong Chian School of Medicine under the Dean's Postdoctoral Fellowship, and the Wong Peng Onn Fellowship (002823-00001).

1. W. Eder, M. J. Ege, E. von Mutius, The asthma epidemic. *N. Engl. J. Med.* **355**, 2226–2235 (2006).
2. B. N. Lambrecht, H. Hammad, The immunology of asthma. *Nat. Immunol.* **16**, 45–56 (2015).
3. Y. Kikuchi *et al*., Crucial commitment of proteolytic activity of a purified recombinant major house dust mite allergen Der p1 to sensitization toward IgE and IgG responses. *J. Immunol.* **177**, 1609–1617 (2006).
4. H. Hammad *et al*., House dust mite allergen induces asthma via Toll-like receptor 4 triggering of airway structural cells. *Nat. Med.* **15**, 410–416 (2009).
5. G. K. Newton *et al*., The discovery of potent, selective, and reversible inhibitors of the house dust mite peptidase allergen Der p 1: An innovative approach to the treatment of allergic asthma. *J. Med. Chem.* **57**, 9447–9462 (2014).
6. I. Sporik, S. T. Holgate, T. A. E. Platts-Mills, J. J. Cogswell, Exposure to house-dust allergen (Der p1) and the development of asthma in childhood. *N. Engl. J. Med.* **323**, 502–507 (1990).
7. L. A. Reynolds, B. B. Finlay, Early life factors that affect allergy development. *Nat. Rev. Immunol.* **17**, 518–528 (2017).
8. E. von Mutius, D. Vercelli, Farm living: Effects on childhood asthma and allergy. *Nat. Rev. Immunol.* **10**, 861–868 (2010). Correction in: *Nat. Rev. Immunol.* **19**, 594 (2019).
9. J. Riedler *et al*.; ALEX Study Team, Exposure to farming in early life and development of asthma and allergy: A cross-sectional survey. *Lancet* **358**, 1129–1133 (2001).
10. M. J. Ege *et al*.; GABRIELA Transregio 22 Study Group, Exposure to environmental microorganisms and childhood asthma. *N. Engl. J. Med.* **364**, 701–709 (2011).
11. M. J. Schuijs *et al*., Farm dust and endotoxin protect against allergy through A20 induction in lung epithelial cells. *Science* **349**, 1106–1110 (2015).
12. E. G. Lee *et al*., Failure to regulate TNF-induced NF-kappaB and cell death responses in A20-deficient mice. *Science* **289**, 2350–2354 (2000).
13. M.-C. Arrieta *et al*.; CHILD Study Investigators, Early infancy microbial and metabolic alterations affect risk of childhood asthma. *Sci. Transl. Med.* **7**, 307ra152 (2015).
14. L.-I. McCall *et al*., Home chemical and microbial transitions across urbanization. *Nat. Microbiol.* **5**, 108–115 (2020).
15. A. B. Lindstrom, M. J. Strynar, E. L. Libelo, Polyfluorinated compounds: Past, present, and future. *Environ. Sci. Technol.* **45**, 7954–7961 (2011).
16. G. W. Olsen *et al*., Half-life of serum elimination of perfluorooctanesulfonate, perfluorohexanesulfonate, and perfluorooctanoate in retired fluorochemical production workers. *Environ. Health Perspect.* **115**, 1298–1305 (2007).
17. M. Houde, J. W. Martin, R. J. Letcher, K. R. Solomon, D. C. Muir, Biological monitoring of polyfluoroalkyl substances: A review. *Environ. Sci. Technol.* **40**, 3463–3473 (2006).
18. "Technical fact sheet–Perfluorooctane sulfonate (PFOS) and perfluorooctanoic acid (PFOA)" (EPA 505-F-17-001, United States Environmental Protection Agency, 2017).
19. A. M. Calafat *et al*., Serum concentrations of 11 polyfluoroalkyl compounds in the u.s. population: Data from the national health and nutrition examination survey (NHANES). *Environ. Sci. Technol.* **41**, 2237–2242 (2007).
20. K. Kato *et al*., Polyfluoroalkyl compounds in pooled sera from children participating in the National Health and Nutrition Examination Survey 2001-2002. *Environ. Sci. Technol.* **43**, 2641–2647 (2009).
21. D. Trudel *et al*., Estimating consumer exposure to PFOS and PFOA. *Risk Anal.* **28**, 251–269 (2008).
22. K. Gao *et al*., Prenatal exposure to per- and polyfluoroalkyl substances (PFASs) and association between the placental transfer efficiencies and dissociation constant of serum proteins-PFAS complexes. *Environ. Sci. Technol.* **53**, 6529–6538 (2019).
23. R. Vestergren, I. T. Cousins, Tracking the pathways of human exposure to perfluorocarboxylates. *Environ. Sci. Technol.* **43**, 5565–5575 (2009).
24. P. Grandjean *et al*., Serum vaccine antibody concentrations in children exposed to perfluorinated compounds. *JAMA* **307**, 391–397 (2012). Correction in: *JAMA* **307**, 1142 (2012).
25. O. Humblet, L. G. Diaz-Ramirez, J. R. Balmes, S. M. Pinney, R. A. Hiatt, Perfluoroalkyl chemicals and asthma among children 12-19 years of age: NHANES (1999-2008). *Environ. Health Perspect.* **122**, 1129–1133 (2014).
26. G.-H. Dong *et al*., Serum polyfluoroalkyl concentrations, asthma outcomes, and immunological markers in a case-control study of Taiwanese children. *Environ. Health Perspect.* **121**, 507–513 (2013).
27. G.-H. Dong *et al*., Sub-chronic effect of perfluorooctanesulfonate (PFOS) on the balance of type 1 and type 2 cytokine in adult C57BL6 mice. *Arch. Toxicol.* **85**, 1235–1244 (2011).
28. E. Corsini, R. W. Luebke, D. R. Germolec, J. C. DeWitt, Perfluorinated compounds: Emerging POPs with potential immunotoxicity. *Toxicol. Lett.* **230**, 263–270 (2014).
29. Y. J. Huang, H. A. Boushey, The microbiome in asthma. *J. Allergy Clin. Immunol.* **135**, 25–30 (2015).
30. C. W. Noorlander, S. P. van Leeuwen, J. D. Te Biesebeek, M. J. Mengelers, M. J. Zeilmaker, Levels of perfluorinated compounds in food and dietary intake of PFOS and PFOA in the Netherlands. *J. Agric. Food Chem.* **59**, 7496–7505 (2011).
31. M. Plantinga *et al*., Conventional and monocyte-derived CD11b(+) dendritic cells initiate and maintain T helper 2 cell-mediated immunity to house dust mite allergen. *Immunity* **38**, 322–335 (2013).
32. G. Qian *et al*., LPS inactivation by a host lipase allows lung epithelial cell sensitization for allergic asthma. *J. Exp. Med.* **215**, 2397–2412 (2018).
33. B. N. Lambrecht, H. Hammad, The airway epithelium in asthma. *Nat. Med.* **18**, 684–692 (2012).
34. L. R. Bonser, D. J. Erle, Airway mucus and asthma: The role of MUC5AC and MUC5B. *J. Clin. Med.* **6**, 112 (2017).
35. M. B. Rosen *et al*., Gene expression profiling in the liver and lung of perfluorooctane sulfonate-exposed mouse fetuses: Comparison to changes induced by exposure to perfluorooctanoic acid. *Reprod. Toxicol.* **27**, 278–288 (2009).
36. L. Ye *et al*., Gene expression profiling in fetal rat lung during gestational perfluorooctane sulfonate exposure. *Toxicol. Lett.* **209**, 270–276 (2012).
37. K. M. Kengatharan, S. De Kimpe, C. Robson, S. J. Foster, C. Thiemermann, Mechanism of gram-positive shock: Identification of peptidoglycan and lipoteichoic acid moieties essential in the induction of nitric oxide synthase, shock, and multiple organ failure. *J. Exp. Med.* **188**, 305–315 (1998).
38. M. Oztug, D. Martinon, P. M. M. Weers, Characterization of the apoLp-III/LPS complex: Insight into the mode of binding interaction. *Biochemistry* **51**, 6220–6227 (2012).
39. B. D. Abbott, Review of the expression of peroxisome proliferator-activated receptors alpha (PPAR alpha), beta (PPAR beta), and gamma (PPAR gamma) in rodent and human development. *Reprod. Toxicol.* **27**, 246–257 (2009).
40. W. K. Midodzi, B. H. Rowe, C. M. Majaesic, L. D. Saunders, A. Senthilselvan, Early life factors associated with incidence of physician-diagnosed asthma in preschool children: Results from the Canadian Early childhood development cohort study. *J. Asthma* **47**, 7–13 (2010).
41. J.-F. Bach, The hygiene hypothesis in autoimmunity: The role of pathogens and commensals. *Nat. Rev. Immunol.* **18**, 105–120 (2018).
42. P. Soroosh *et al*., Lung-resident tissue macrophages generate Foxp3+ regulatory T cells and promote airway tolerance. *J. Exp. Med.* **210**, 775–788 (2013).
43. J. Saravia *et al*., Early-life exposure to combustion-derived particulate matter causes pulmonary immunosuppression. *Mucosal Immunol.* **7**, 694–704 (2014).
44. G.-H. Dong *et al*., Subchronic effects of perfluorooctanesulfonate exposure on inflammation in adult male C57BL/6 mice. *Environ. Toxicol.* **27**, 285–296 (2012).
45. C. A. Ng, K. Hungerbühler, Bioaccumulation of perfluorinated alkyl acids: Observations and models. *Environ. Sci. Technol.* **48**, 4637–4648 (2014).
46. S. Beesoon, J. W. Martin, Isomer-specific binding affinity of perfluorooctanesulfonate (PFOS) and perfluorooctanoate (PFOA) to serum proteins. *Environ. Sci. Technol.* **49**, 5722–5731 (2015).
47. C. Ng, M. Khazaee, J. Field, E. Christie, M. Michalsen, "Molecular Design of Effective and Versatile Adsorbents for Ex Situ Treatment of AFFF-Impacted Groundwater" (Tech. Rep. ER-181417 US Army Engineer Research Development Center, 2019).
48. Y. Liu, Z. Cao, W. Zong, R. Liu, Interaction rule and mechanism of perfluoroalkyl sulfonates containing different carbon chains with human serum albumin. *RSC Advances* **7**, 24781–24788 (2017).
49. D. J. Luebker, K. J. Hansen, N. M. Bass, J. L. Butenhoff, A. M. Seacat, Interactions of fluorochemicals with rat liver fatty acid-binding protein. *Toxicology* **176**, 175–185 (2002).
50. E. Corsini *et al*., In vitro characterization of the immunotoxic potential of several perfluorinated compounds (PFCs). *Toxicol. Appl. Pharmacol.* **258**, 248–255 (2012).

Downloaded at University of Liverpool on September 20, 2021

51. E. Corsini *et al*., In vitro evaluation of the immunotoxic potential of perfluorinated compounds (PFCs). *Toxicol. Appl. Pharmacol.* **250**, 108–116 (2011).
52. K. Midgett, M. M. Peden-Adams, G. S. Gilkeson, D. L. Kamen, In vitro evaluation of the effects of perfluorooctanesulfonic acid (PFOS) and perfluorooctanoic acid (PFOA) on IL-2 production in human T-cells. *J. Appl. Toxicol.* **35**, 459–465 (2015).
53. J. C. DeWitt *et al*., Immunotoxicity of perfluorooctanoic acid and perfluorooctane sulfonate and the role of peroxisome proliferator-activated receptor alpha. *Crit. Rev. Toxicol.* **39**, 76–94 (2009).
54. M. E. Andersen *et al*., Perfluoroalkyl acids and related chemistries–Toxicokinetics and modes of action. *Toxicol. Sci.* **102**, 3–14 (2008).
55. J. C. DeWitt, M. M. Peden-Adams, J. M. Keller, D. R. Germolec, Immunotoxicity of perfluorinated compounds: Recent developments. *Toxicol. Pathol.* **40**, 300–311 (2012).
56. C. Suo, Z. Fan, L. Zhou, J. Qiu, Perfluorooctane sulfonate affects intestinal immunity against bacterial infection. *Sci. Rep.* **7**, 5166 (2017).
57. L. Torres *et al*., Effect of Perfluorooctanesulfonic acid (PFOS) on immune cell development and function in mice. *Immun. Letters* **233**, 31–41 (2021).
58. M. Fang, T. F. Webster, P. L. Ferguson, H. M. Stapleton, Characterizing the peroxisome proliferator-activated receptor (PPARγ) ligand binding potential of several major flame retardants, their metabolites, and chemical mixtures in house dust. *Environ. Health Perspect.* **123**, 166–172 (2015).
59. M. Lorber, P. P. Egeghy, Simple intake and pharmacokinetic modeling to characterize exposure of Americans to perfluoroctanoic acid, PFOA. *Environ. Sci. Technol.* **45**, 8006–8014 (2011).
60. M. M. Stein *et al*., Innate immunity and asthma risk in Amish and Hutterite farm children. *N. Engl. J. Med.* **375**, 411–421 (2016).
61. K. F. Budden *et al*., Emerging pathogenic links between microbiota and the gut-lung axis. *Nat. Rev. Microbiol.* **15**, 55–63 (2017).
62. E. d'Hennezel, S. Abubucker, L. O. Murphy, T. W. Cullen, Total lipopolysaccharide from the human gut microbiome silences toll-like receptor signaling. *mSystems* **2**, e00046-17 (2017).
63. M. Lu *et al*., Stimulus-dependent deacylation of bacterial lipopolysaccharide by dendritic cells. *J. Exp. Med.* **197**, 1745–1754 (2003).
64. F. Pérez *et al*., Accumulation of perfluoroalkyl substances in human tissues. *Environ. Int.* **59**, 354–362 (2013).
65. Environmental Working Group, Report: Up to 110 million Americans could have PFAS-contaminated drinking water-PFAS tap water data was funded by Taxpayers but kept secret. (2018). https://www.ewg.org/research/report-110-million-americans-could-have-pfas-contaminated-drinking-water. Accessed 10 May 2020.

Downloaded at University of Liverpool on September 20, 2021